Experimental pilot study for augmented reality-enhanced elbow arthroscopy

Michiro Yamamoto (michi-ya@med.nagoya-u.ac.jp)
Nagoya University https://orcid.org/0000-0002-6753-538X
Shintaro Oyama
Nagoya University
Syuto Otsuka
Riken Center for Advanced Photonics
Yukimi Murakami
RIKEN Center for Advanced Photonics
Hideo Yokota
RIKEN Center for Advanced Photonics
Hitoshi Hirata
Nagoya University

Research article

Keywords: augmented reality, elbow, arthroscopy

Posted Date: June 19th, 2020

DOI: https://doi.org/10.21203/rs.3.rs-35552/v1

Version of Record: A version of this preprint was published at Scientific Reports on February 25th, 2021.
See the published version at https://doi.org/10.1038/s41598-021-84062-7.

Experimental pilot study for augmented reality-enhanced elbow arthroscopy

Michiro Yamamoto, MD, PhD[1], Shintaro Oyama, MD, PhD[1], Syuto Otsuka[2,3],

Yukimi Murakami, PhD[3], Hideo Yokota, PhD[3], Hitoshi Hirata, MD, PhD[1]

1) Department of Hand Surgery, Nagoya University, Japan

2) Department of Mechanical Engineering, Tokyo university of Science

3) Image Processing Research Team, RIKEN Center for Advanced Photonics, Japan

Address correspondence to: Michiro Yamamoto

Department of Hand Surgery Nagoya University Graduate School of Medicine

65 Tsurumai-cho, Showa-ku, Nagoya 466-8550, Japan

Tel: +81-52-744-2957; Fax: +81-52-744-2964

E-mail: michi-ya@med.nagoya-u.ac.jp

Running title; Augmented reality-enhanced elbow arthroscopy

Abstract

Background: The purpose of this study was to develop and evaluate a novel elbow arthroscopy system with superimposed bone and nerve visualization based on preoperative computed tomography (CT) and magnetic resonance imaging (MRI) data.

Methods: We obtained bone and nerve segmentation data by CT and MRI, respectively, of the elbow of a healthy human volunteer and cadaveric Japanese monkey. A life size 3-dimensional (3D) model of human organs and frame was constructed using a stereo-lithographic 3D printer. Elbow arthroscopy was performed using the elbow of a cadaveric Japanese monkey. The augmented reality (AR) range of error was examined at 1 cm and 2 cm scope–object distances.

Results: We successfully performed AR arthroscopy using the life-size 3D elbow model and the elbow of the cadaveric Japanese monkey by making anteromedial and posterior portals. The computer graphics (CG) position and shape were initially different because of lens distortion. The CG position and shape were corrected to match the arthroscopic view using lens distortion parameter estimates based on the calibration pattern. AR position and shape errors were 2.3 mm at 1 cm scope–object distance and 3.6 mm at 2 cm scope–object distance.

Conclusion: We attained reasonable accuracy and demonstrated the working of the

designed system. Given the multiple applications of AR-enhanced arthroscopic visualization, it has the potential to be the next-generation technology for arthroscopy. This technique will contribute the reduction of serious complications associated with elbow arthroscopy.

Keywords augmented reality, elbow, arthroscopy

Background

Available evidence supports use of elbow arthroscopy to manage multiple conditions including rheumatoid arthritis, osteoarthritis, tennis elbow, and osteochondritis dissents. A major drawback of elbow arthroscopy is the risk of intraoperative complications, including serious neurovascular injuries[1]. The small working space and near adjacency of neurovascular and arthroscopic portals make elbow arthroscopy a technically demanding procedure. Successful elbow arthroscopy requires extensive knowledge of the spatial correlations among the neurovasculature, entry portals and joint structures.

Recent advancements in sophisticated image processing technology have made precise preoperative simulations a possibility, and they are becoming increasingly common in clinical practice[2]. But this valuable set of information is ineffectively utilized in elbow arthroscopy at arguably the most decisive point: during the procedure[3]. The ability to access such data that is optimized for use and seamlessly integrated into the surgical navigation system has remained elusive. We propose that the safety of standard elbow arthroscopy can be improved by incorporating augmented reality (AR). AR can allow delivery of selective complex and highly useful information through computer graphics (CG) superimposed onto real-time video.

The purpose of this study is to develop and evaluate a novel elbow arthroscopy system with superimposed bone and nerve visualizations based on computed tomography (CT) and magnetic resonance imaging (MRI) data. We hypothesize that the accuracy of the resulting AR enhancement to standard arthroscopy would be acceptable.

Methods

This study was conducted under the approval of local institutional review board.

Experiment 1.

Data collection, processing and 3-dimensional (3D) modeling of body organs

Skin, bone, and nerve segmentation data of the elbow of a healthy human volunteer were obtained by CT and MRI, respectively. Inter-modal voxel registration was performed using ANT software with a SyN non-linear registration algorithm and affin registration[4]. Segmentation and refinement were performed using VoTracer software (Riken, Wako, Japan, http://www.riken.jp/brict/Ijiri/VoTracer/)[5]. All segmented lesion data were exported as Standard Triangulated Language (STL) data.

We added support frame STL data to correctly coordinate bones and nerves upon 3D printing and printed a life size 3D model of organs and frame using a stereo-lithographic 3D printer (Object500 Connex, Stratasys Ltd, US.). (Fig. 1)

Setup of elbow arthroscopy and device tracking system.

We used a tracking system (MicronTracker3; ClaroNav, Toronto, Canada) for surgical device tracking. MicronTracker3 is an optical pose tracking system with a unique ability to track an unlimited number of tools simultaneously.

Each tracking marker used in the system was composed of black and white regions and system computed target locations at the intersection of four high-contrast regions. Each of the four black and white boundary lines independently served to pinpoint the location of targets called ‘Xpoints’.

Unlike bright spot markers, Xpoints have information on location and orientation. This additional discriminating characteristic greatly reduces erroneous mismatches between targets on left and right images. It also reduces marker misidentification, as matching the characteristics of the observed targets against templates leads to identification. As misleading bright reflection spots are more common in an operating environment compared with Xpoints, the use of Xpoints greatly reduces the risk of misidentification.

The markers were identified with reference to a marker template database, and allowed distinguishing between multiple different instruments. Furthermore, the database

109 can be updated during run-time, allowing new marker templates to be added simply by
110 presenting them to the camera and assigning a name to them. We placed different markers
111 onto each 3D model baseplate and used the arthroscopy camera for tracking. To stabilize
112 markers on the arthroscopy camera, we made custom stainless-steel guides that could
113 attach markers on the arthroscope. (Fig. 2a)
114
115 Augmented reality image processing during training surgery
116 While performing elbow arthroscopy on the generated 3D model, an AR
117 calculated CG image was superimposed onto the arthroscopic video view by our AR
118 system.
119 The system summary is as follows (Fig. 2b).
120
121 1. Arthroscopy image data were captured on the computer through a digital video
122 capture card connected to the arthroscopy camera system.
123 2. The data of the 3D model base plate and the arthroscopy camera body loci were
124 provided by MicronTracker3, which was able to trace target information using a
125 customized software developed using the MicronTracker software developers' kit.
126 Coordination system of the 3D model of organs and the arthroscopy camera were

127 defined as $\Sigma_{\square}$ and $\Sigma_{\square}$. Transformation matrix from MicronTracker3 sensor ($\square_{\square}$) to the

128 marker reference point (fiducial point) of $\Sigma_{\square}$: ($\square_{\square 0} = \Sigma_{\square(x,y,z=0,0,0)}$) and Σ_A: ($\square_{\square 0} =$

129 $\Sigma_{\square(x,y,z=0,0,0)}$) was found by stereo-triangulating the optical marker defined as $\square_{\square\square}$

130 and $\square_{\square\square}$. Transformation matrix from $\square_{\square 0}$ to each organ STL model reference point

131 $\square_{\square}$ was pre-defined as $\square_{\square\square}$ (Though organ models include skin, radius, ulna, humerus,

132 radial nerve, ulnar nerve, median nerve, musculocutaneous nerve, and they were

133 handled separately in calculation, 3D relationship between these models are static,

134 therefore the reference point of these models were expressed as single point in this

135 expression ($\square_{\square}$)), and $\square_{\square 0}$ to the tip of arthroscopy light rod $\square_{\square}$ was pre-defined as

136 $\square_{\square\square}$ before examination.

137 3. Our custom-made software installed on the computer calculated each 3D organ model

138 and arthroscopy light fiber rod position and direction. Position of virtual camera was

139 placed on $\square_{\square}$ and rotated according to the lens-offset angle (In this experiment, it was

140 30 degrees.); therefore the coordination system of camera sight $\Sigma_{\square}$ must consider this

141 angle.

142 Calculation to transform $\Sigma_{\square}$ to $\Sigma_{\square}$ is as follows;

144 $$\Sigma_{\square} = \square_{\square\square}\Sigma_A = \frac{\square_{\square\square}}{\square_{\square\square}}\Sigma_{\square}$$

143 Each 3D organ model data was rendered according to this transformation. A

145 homogenous transformation can be constructed to register the virtual arthroscopy
146 view to the real arthroscopy view. This calculation was performed with the assistance
147 of OpenCV software (Intel, US).
148 4. The rendered image 3 was superimposed on the image 1 and displayed on the monitor.
149
150 **Experiment 2**
151 Data collection, processing and 3D modeling of organs
152 Elbow (1/2 of upper arm ~ 1/2 of forearm) of a Japanese monkey cadaver was
153 used for this experiment. The X-ray CT data of the cadaveric elbow was used with
154 modeled frame data that could be precisely attached to the humerus and ulna on the
155 posture at 90 degrees elbow flexion, 90 degrees forearm pronation. The frame was printed
156 on a 3D printer (Davinci 1.0A / XYZ Printing, Inc. US.) using Acrylonitrile butadiene
157 styrene plastic. The frame was then fixed to the cadaver elbow with epoxy resin to ensure
158 that it could not be easily moved. (Fig. 3a)
159 X-ray CT and MRI of elbow and the frame were performed and these datasets
160 were used to obtain the bone and nerve data using methods similar to experiment 1. We
161 obtained bone segmentation from the CT data and nerve segmentation from the MRI data
162 of a cadaveric Japanese monkey elbow. Segmentation and refinement were performed

using the VoTracer software (Riken, Wako, Japan). All segmented lesion data was exported as STL data. (Fig. 3b)

Setup of elbow arthroscope and device tracking system.

Tracking system setup was similar to experiment 1 except that we added an anti-pollution barrier on the system. Washable stainless-steel base plate was constructed to stabilize the elbow frame, and placed at different markers on the baseplate and the arthroscopy camera head. Relative position between the baseplate and elbow frame was static. 3D model base plate and arthroscopy camera body loci data was provided by MicronTracker3. The rendered images were superimposed on the real-time view and displayed on the AR monitor.

Augmented reality image processing during training surgery

Elbow arthroscopy surgery was performed on the monkey elbow through anteromedial and posterior portals. While operating on the cadaver elbow, AR calculated C image was superimposed onto the arthroscopic video by the same method as described in experiment 1. Reverse distortion correlation was performed using lens distortion matrix. The matrix was pre-calculated using calibration pattern of arthroscopy camera.

AR position error calculation

The AR range of error was examined to evaluate the accuracy of the AR system. A checkerboard and marker were superimposed to calculate the range of error. A checkerboard printed on a cardboard and a pre-settled virtual marker were superimposed to calculate registration errors. Distances between the centers of the markers were set to be same as the checkerboard lattice span, and the precision of the super-imposement were examined at 1 cm and 2 cm scope-object distances (Fig.4).

Results

We successfully performed AR arthroscopy for the full-size 3D elbow model. The CG data was superimposed onto the elbow arthroscopy video in real-time. We performed a registration to co-visualize the image of the patient's elbow structures and the CG made using preoperative images. After manual modification of the position, scale, and orientation, the accuracy of the superimposed CG data was deemed acceptable on the AR monitor.

AR arthroscopy of the cadaveric Japanese monkey elbow was performed (Fig.5a). Humeroradial joint and Radial nerve were superimposed on the real-time view and

showed on the AR monitor. Although Radial nerve was not seen on the scope monitor as it was located behind the joint capsule, the position of the radial nerve was clearly observed. This was helpful to the surgeon in creating a lateral portal thereby avoiding radial nerve injury (Fig. 5b).

The CG position and shape were initially different due to lens distortion. However, the CG position and shape were corrected to match the arthroscopic view using lens distortion parameters, which were estimated from the calibration pattern in experiment 2 (Fig. 6). The AR position and shape errors were 2.3 mm at 1 cm scope–object distance and 3.6 mm at 2 cm scope-object distance.

Discussion

We have successfully integrated AR technology with elbow arthroscopy. We have demonstrated the workings of the system and the accuracy of this AR system was deemed satisfactory. Through further iterations and refinements, AR-enhanced arthroscopic visualization has the potential to be a transformative technology. This technique will contribute in reducing the risk of serious complications associated with elbow arthroscopy.

The rapid development of endoscopy has enabled minimally invasive surgeries. However, this technique has a spatial perception disadvantage. The surgeon needs to

alternate between the macroscopic view of the surgical field and the endoscopic view. AR navigation has recently been employed during brain, spinal, plastic, maxillofacial, and several other highly technically demanding surgeries[6-8]. However, few studies have focused on its use in upper limb arthroscopy[9]. There is an unmet need for the next-generation arthroscopy system especially designed for the elbow, due to high incidences of associated intraoperative complications.

Creating AR-enhanced navigation requires 3D preoperative imaging of the target tissue, AR display, tracking system, and a software to calculate the arthroscopy position and direction for each 3D organ.

VoTracer is software employed for volume computer aided design (VCAD) of pre-operative CT and MRI data. Segmentation and refinement of bones and nerves data can be performed using this software. A limitation associated with all VCAD softwares is the need for manual work in creating CG of the target tissue. Fine anatomical knowledge of the elbow, especially of nerve route is required to complete segmentation and refinement of the tissues.

There are several methods of display for AR. See-through glasses and 3D projection mapping are possible AR displays. See-through glasses have a drawback that it is difficult to obtain an accurate AR view superimposed on the real view. The see-

through glasses need to track the pupil positions in real-time for registration. 3D projection mapping is another way to display AR view. In order to obtain an AR view on the patient skin, the video projector has to be set over the patient in the operating room. As both deep and superficial structures are displayed on the skin surface, a significant error of perception is noted when more than two surgeons see the AR display[7]. We employed a video-based display with two monitors for real arthroscopic view and the AR-enhanced view. This system was a natural fit for arthroscopy as the surgeon could simultaneously confirm the real and AR-enhanced view.

A variety of tracking systems are available for clinical settings e.g. infrared camera-based tracking, the tag video tracking, and electromagnetic tracking[10,11]. Accuracy of the tracking device is very important in clinic as it is directly linked to safety. We used an optical tracking device, MicronTracker3. It was able to trace each target information in real-time using a customized software developers' kit. Accuracy of this tracking system was deemed acceptable and the position and shape error was 2.3 mm at a 1 cm scope-object distance.

Arthroscopy simulator training improves performance of students and residents during knee and shoulder surgery[12-14]. Recently, multiple types of virtual reality based training simulators for arthroscopy have been reported[15]. Among those simulators, high-

253 fidelity virtual reality simulation was reported to be superior compared to the low-fidelity
254 model to acquire arthroscopic skills[16]. AR enhanced arthroscopic system with
255 superimposed tasks can be a high-fidelity training tool for surgical education. This system
256 can also provide a third person view using the stereo camera on the optical tracking device,
257 MicronTracker3. Third person view and record of tracking makers provide a trainee
258 feedback regarding handling of scope and other instruments during surgery.

259 AR enhanced navigation for arthroscopy may become the next generation
260 arthroscopy system. However, there are some limitations in this study. First, we used
261 preoperative imaging techniques such as CT and MRI but not real-time information of
262 the target tissue. The size and location of the lesion at the time of surgery may differ from
263 preoperative data. Second, the elbow flexion angle was fixed in our experiments, however
264 surgeons in a clinical setting typically move the elbow during arthroscopy. Superimposed
265 CG data therefore needs to change according to the elbow angle. AR with real-time data
266 of the target tissue is required to solve these problems. Intraoperative CT, MRI, or
267 ultrasonography may be employed to obtain intraoperative data of the target tissue.
268 Actually, nerves around the elbow can be clearly visualized using ultrasonography[17,18]. In
269 addition algorithm for intraoperative data is required.

270

Conclusions

The technological integration of AR with arthroscopy was successful. We attained satisfactory accuracy and demonstrated the workings of such a system. Upon resolution of some limitations, the AR-enhanced arthroscopic visualization has the potential to become the next-generation arthroscopy. Elbow arthroscopy procedure requires significant training for surgeons, and even skilled surgeons have reported complications during surgery. We believe that AR-enhanced arthroscopy will reduce the risk of serious complications associated with elbow arthroscopy.

Abbreviations

AR: augmented reality

CT: computed tomography

MRI: magnetic resonance imaging

3D; 3-dimensional

CG: computer graphics

STL: Standard Triangulated Language

VCAD: volume computer aided design

References

1. Desai MJ, Mithani SK, Lodha SJ, Richard MJ, Leversedge FJ, Ruch DS. Major Peripheral Nerve Injuries After Elbow Arthroscopy. Arthroscopy. 2016;32(6):999-1002.e1008.

2. Yamamoto M, Murakami Y, Iwatsuki K, Kurimoto S, Hirata H. Feasibility of four-dimensional preoperative simulation for elbow debridement arthroplasty. BMC Musculoskelet Disord. 2016;17:144.

3. Miyake J, Shimada K, Oka K, et al. Arthroscopic debridement in the treatment of patients with osteoarthritis of the elbow, based on computer simulation. Bone Joint J. 2014;96(2):237-41.

4. Avants BB, Tustison N, Song G. Advanced normalization tools (ANTS). Insight j. 2009;2:1-35.

5. Ijiri T, Yokota H. Contour - based Interface for Refining Volume Segmentation. Paper presented at: Computer Graphics Forum2010.

6. Kersten-Oertel M, Gerard I, Drouin S, et al. Augmented reality in neurovascular surgery: feasibility and first uses in the operating room. Int J Comput Assist Radiol Surg. 2015;10(11):1823-36.

7. Nicolau S, Soler L, Mutter D, Marescaux J. Augmented reality in laparoscopic

surgical oncology. Surg Oncol. 2011;20(3):189-201.

8. Shuhaiber JH. Augmented reality in surgery. Arch Surg. 2004;139(2):170-4.

9. Zemirline A, Agnus V, Soler L, Mathoulin CL, Obdeijn M, Liverneaux PA. Augmented reality-based navigation system for wrist arthroscopy: feasibility. J Wrist Surg. 2013;2(4):294-8.

10. Pagador JB, Sánchez L, Sánchez J, Bustos P, Moreno J, Sánchez-Margallo FM. Augmented reality haptic (ARH): an approach of electromagnetic tracking in minimally invasive surgery. Int J Comput Assist Radiol Surg. 2011;6(2):257-63.

11. Teber D, Guven S, Simpfendörfer T, et al. Augmented reality: a new tool to improve surgical accuracy during laparoscopic partial nephrectomy? Preliminary in vitro and in vivo results. Eur Urol. 2009;56(2):332-8.

12. Aim F, Lonjon G, Hannouche D, Nizard R. Effectiveness of Virtual Reality Training in Orthopaedic Surgery. Arthroscopy. 2016;32(1):224-32.

13. Cannon WD, Garrett WE, Jr., Hunter RE, et al. Improving residency training in arthroscopic knee surgery with use of a virtual-reality simulator. A randomized blinded study. J Bone Joint Surg Am. 2014;96(21):1798-806.

14. Rebolledo BJ, Hammann-Scala J, Leali A, Ranawat AS. Arthroscopy skills development with a surgical simulator: a comparative study in orthopaedic surgery

residents. Am J Sports Med. 2015;43(6):1526-9.

15. Vaughan N, Dubey VN, Wainwright TW, Middleton RG. A review of virtual reality based training simulators for orthopaedic surgery. Med Eng Phys. 2016;38(2):59-71.

16. Banaszek D, You D, Chang J, et al. Virtual Reality Compared with Bench-Top Simulation in the Acquisition of Arthroscopic Skill: A Randomized Controlled Trial. J Bone Joint Surg Am. 2017;99(7):e34.

17. McCartney CJ, Xu D, Constantinescu C, Abbas S, Chan VW. Ultrasound examination of peripheral nerves in the forearm. Reg Anesth Pain Med. 2007;32(5):434-9.

18. Heinemeyer O, Reimers CD. Ultrasound of radial, ulnar, median, and sciatic nerves in healthy subjects and patients with hereditary motor and sensory neuropathies. Ultrasound Med Biol. 1999;25(3):481-5.

Declarations

Ethics approval and consent to participate

The study protocol was approved by the Ethics Committee of Nagoya University Hospital (2020-0013). Informed consent was obtained from all participants in this study. All methods in this study were performed in accordance with relevant guidelines and regulations.

Consent for publication

Not applicable.

Availability of data and materials

The datasets during the current study available from the corresponding author on reasonable request.

Competing interests

The authors declare no competing financial and non-financial interests.

Funding

Research reported in this publication was supported by the Japan Society for the Promotion of Science under Award # 26462262 of the Grant-in-Aid for Scientific Research. The contents of this manuscript are the sole responsibility of the authors and do not represent the official views of the Japan Society for the Promotion of Science.

Contributions

MY, SO, and HY have full access to all of the data in the study and take responsibility for the integrity of the data and the accuracy of the data analysis.

Study concept and design: MY and HY

Acquisition of data: MY, SO, SO, and YM

Analysis and interpretation of data: MY and HH.

Drafting of the manuscript: MY and SO

Critical revision of the manuscript for important intellectual content: MY and HH

Administrative, technical, or material support: SO, YM and HY

Study supervision: MY, HH, and HY

All authors have read and approved the final submitted manuscript.

Acknowledgement

None of the authors has received any type of support or benefits from any commercial party related directly or indirectly to the subject of this article.

Figure legends

Fig.1 A real size 3-dimensional (3D) model of organs and frame.

The model was made by using a Standard Triangulated Language (STL) 3D printer (Object500 Connex, Stratasys Ltd, US.).

Fig.2 Elbow arthroscopy and tracking device system.

Red arrows indicate Xpoints (a). The Schema of augmented reality (AR) Arthroscopy System (b).

Fig.3 Elbow of a Japanese monkey cadaver and Standard Triangulated Language (STL) data.

We used the elbow (1/2 of upper arm ~ 1/2 of forearm) of Japanese monkey cadaver. From X-ray computed tomography (CT) data of the cadaveric elbow, we modeled frame data that can be precisely attached to humerus and ulna on the posture of 90 degrees elbow

391 flexion, 90 degrees forearm pronation (a). We obtained bone segmentation from CT data
392 and nerves from magnetic resonance image (MRI) data of a cadaveric Japanese monkey
393 elbow. Segmentation and refinement were performed by using VoTracer software (Riken,
394 Wako, Japan) (b).
395
396 **Fig. 4** Augmented reality (AR) system alignment and registration error calculation and
397 calibration
398 The error distance was examined at 1 cm and 2 cm scope–object distances to determine
399 the effect of viewing distance. A checkerboard and marker were superimposed to
400 calculate error.
401
402 **Fig. 5** Augmented reality (AR) arthroscopy on cadaveric Japanese monkey elbow.
403 Capitellum and radial head were visualized through anteromedial portal and visualized
404 on the scope monitor (a). Humeroradial joint and Radial nerve (white arrows) were
405 superimposed on the real view (b). Red arrow indicates a third person view using the
406 stereo camera on the optical tracking device.
407
408 **Fig. 6** Reverse distortion correction using lens distortion matrix.

White arrows show differences between before and after correction. Appropriate distortion of the shape on the monitor was corrected.

Figures

Figure 1

A real size 3-dimensional (3D) model of organs and frame. The model was made by using a Standard Triangulated Language (STL) 3D printer (Object500 Connex, Stratasys Ltd, US.).

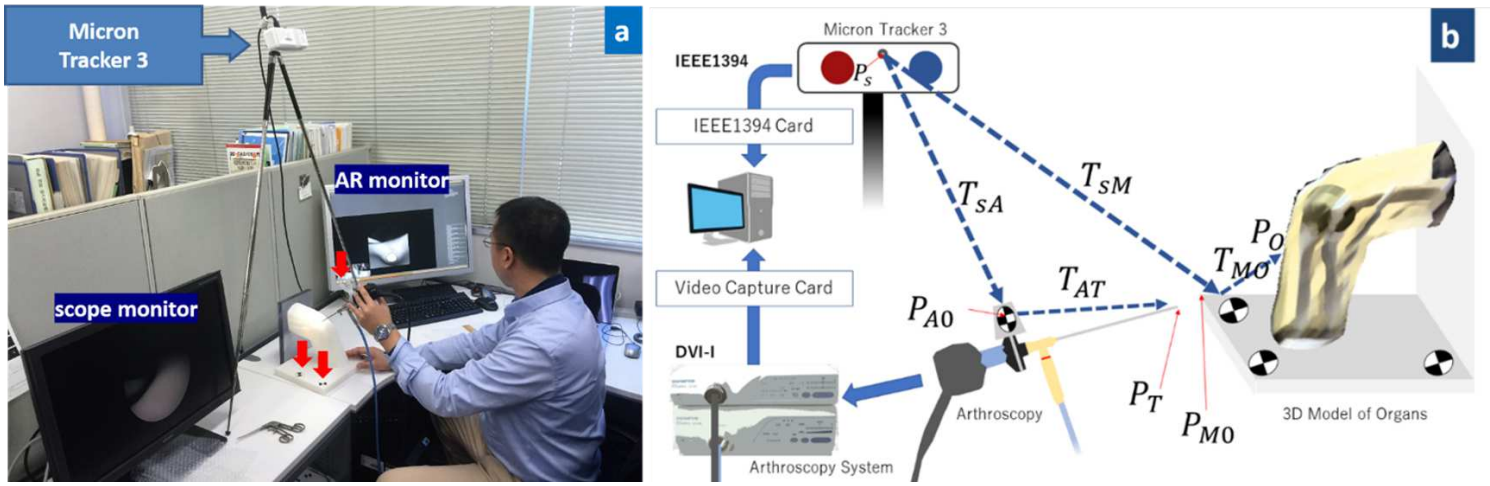

Figure 2

Elbow arthroscopy and tracking device system. Red arrows indicate Xpoints (a). The Schema of augmented reality (AR) Arthroscopy System (b).

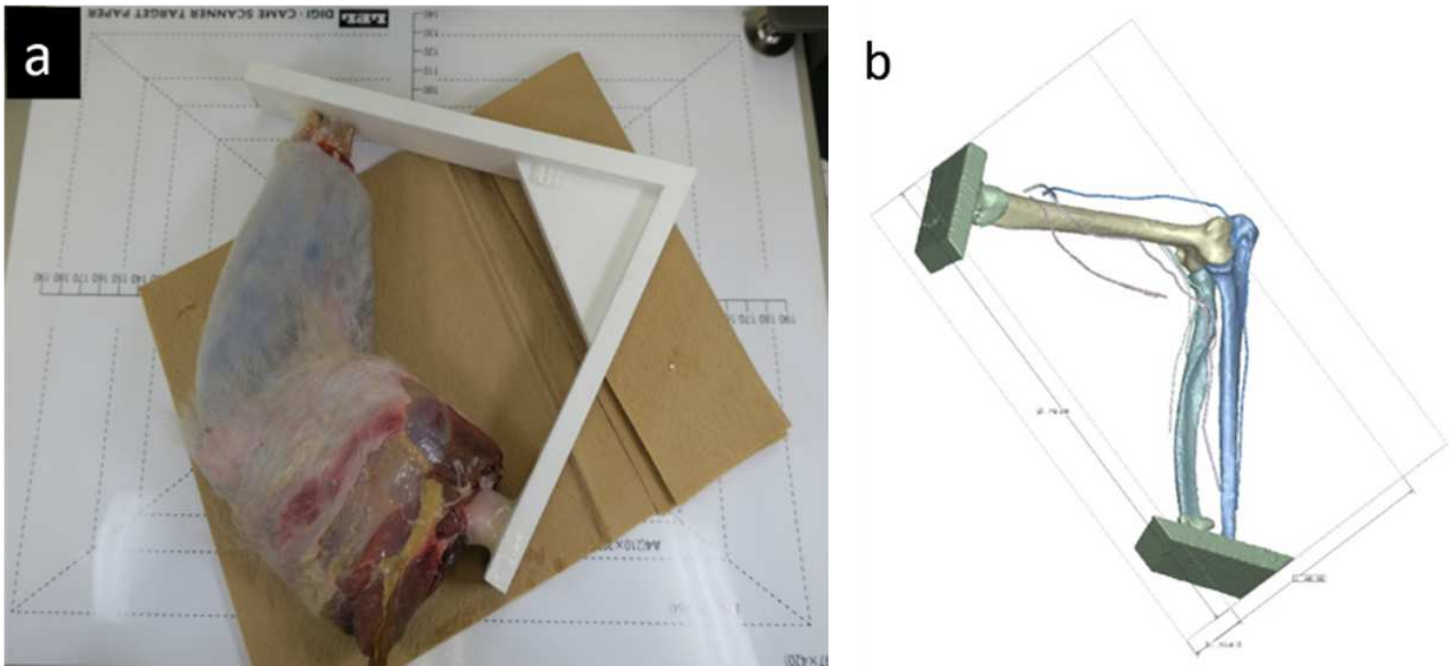

Figure 3

Elbow of a Japanese monkey cadaver and Standard Triangulated Language (STL) data. We used the elbow (1/2 of upper arm ~ 1/2 of forearm) of Japanese monkey cadaver. From X-ray computed tomography (CT) data of the cadaveric elbow, we modeled frame data that can be precisely attached to humerus and ulna on the posture of 90 degrees elbow flexion, 90 degrees forearm pronation (a). We obtained bone segmentation from CT data and nerves from magnetic resonance image (MRI) data of a cadaveric Japanese monkey elbow. Segmentation and refinement were performed by using VoTracer software (Riken, Wako, Japan) (b).

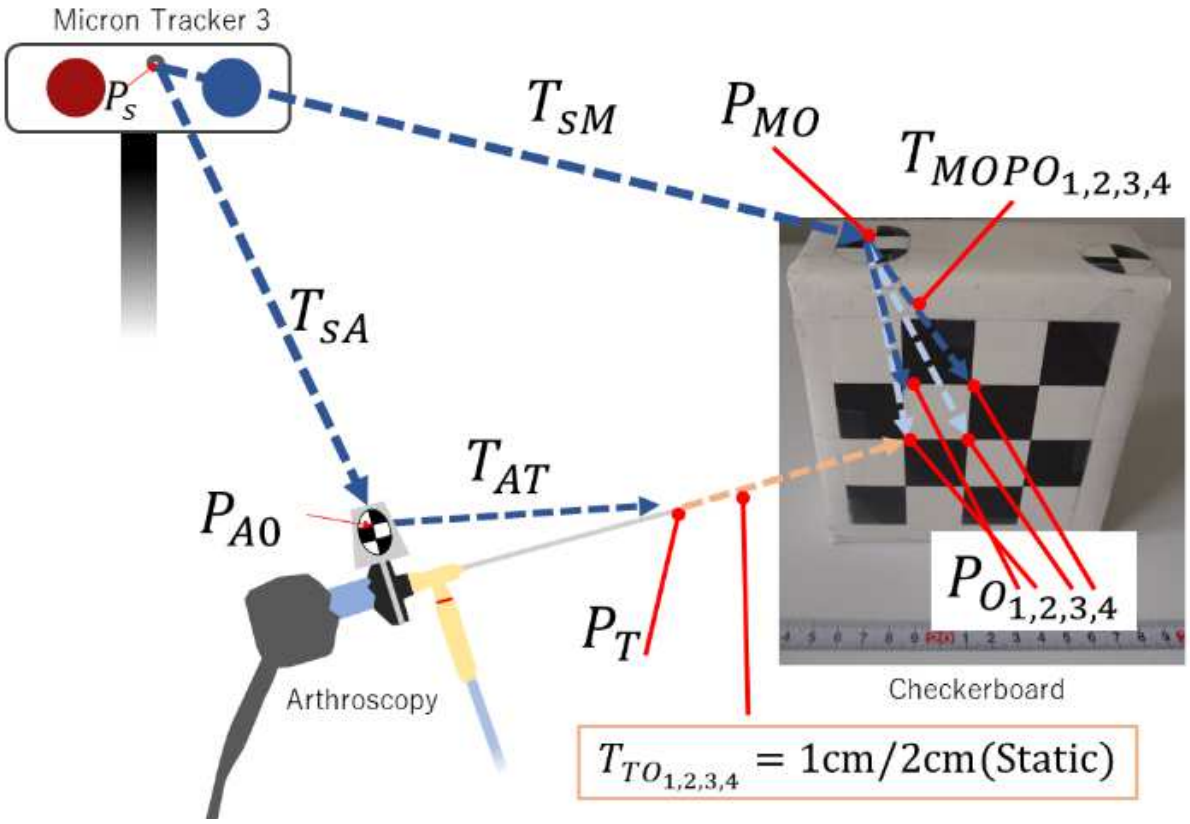

Figure 4

Augmented reality (AR) system alignment and registration error calculation and calibration The error distance was examined at 1 cm and 2 cm scope–object distances to determine the effect of viewing distance. A checkerboard and marker were superimposed to calculate error.

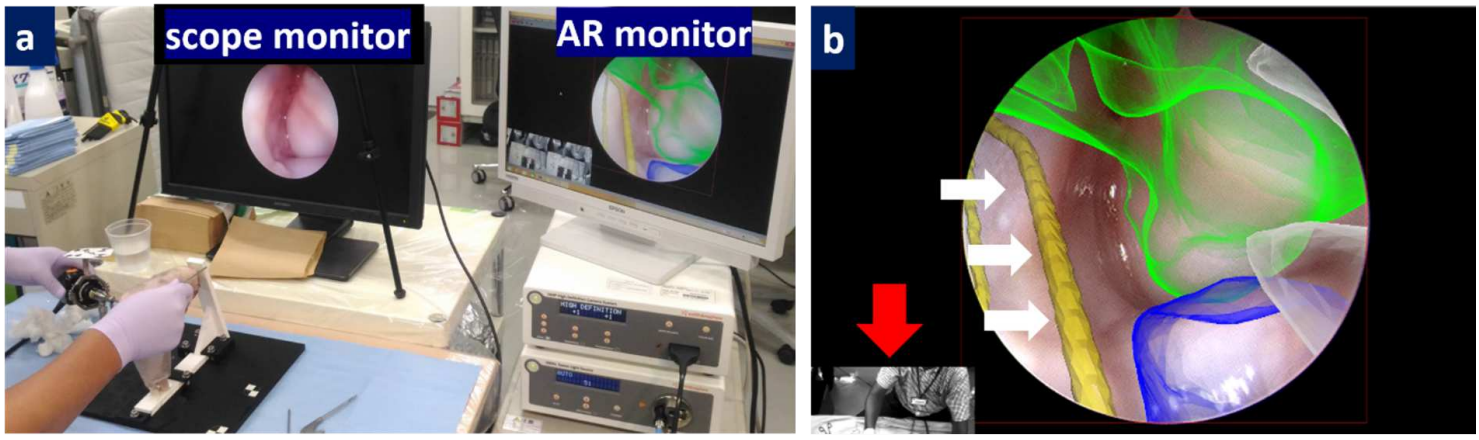

Figure 5

Augmented reality (AR) arthroscopy on cadaveric Japanese monkey elbow. Capitellum and radial head were visualized through anteromedial portal and visualized on the scope monitor (a). Humeroradial joint and Radial nerve (white arrows) were superimposed on the real view (b). Red arrow indicates a third person view using the stereo camera on the optical tracking device.

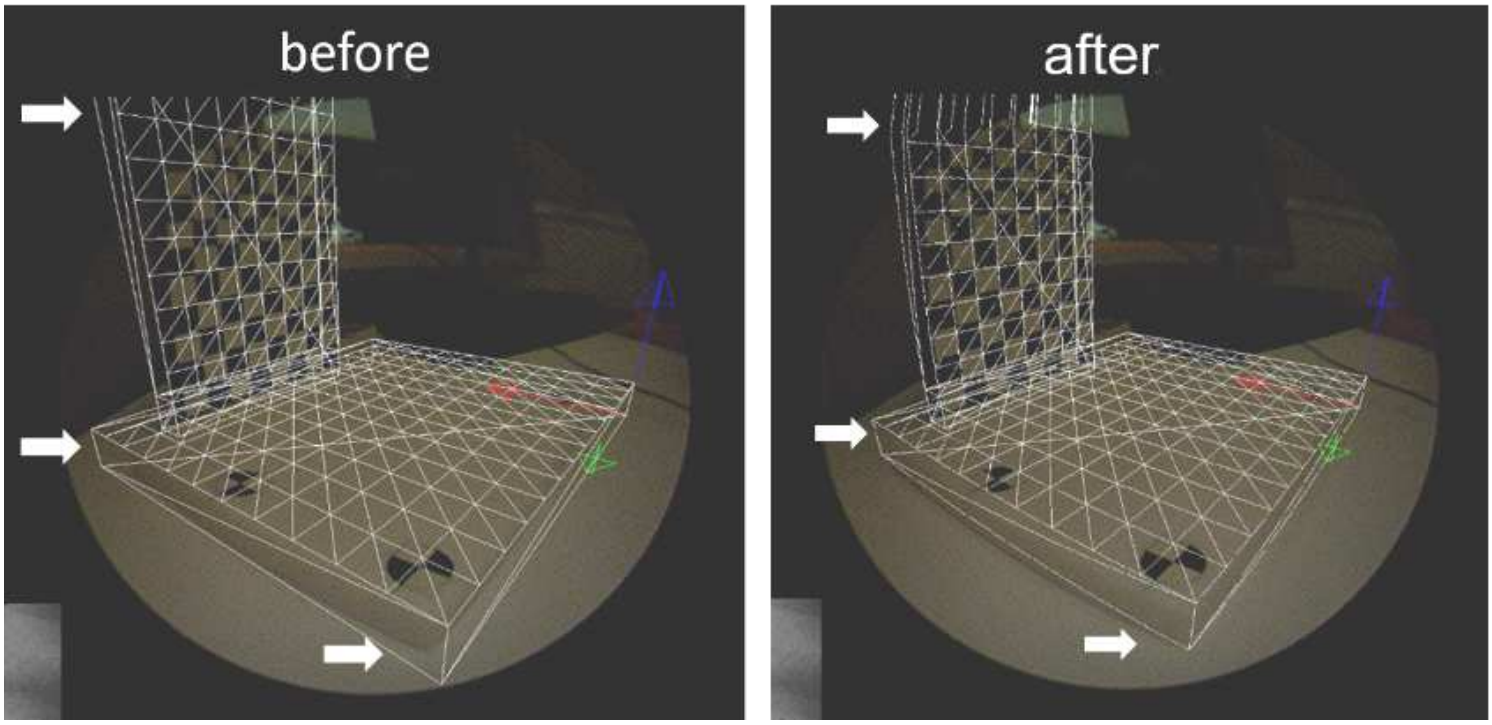

Figure 6

Reverse distortion correction using lens distortion matrix.